



© 2024. The Author(s). This is an open-access article distributed under the terms of the Creative Commons Attribution-ShareAlike 4.0 International Public License (CC BY SA 4.0, <https://creativecommons.org/licenses/by-sa/4.0/legalcode>), which permits use, distribution, and reproduction in any medium, provided that the article is properly cited.

Physicochemical properties of water in the Nida valley, Poland

Cong Ngoc Phan^{1,2*}, Andrzej Strużyński¹, Tomasz Kowalik¹

¹Faculty of Environmental Engineering and Land Surveying, University of Agriculture in Krakow, Poland

²Institute of Chemistry, Biology and Environment, Vinh University, Vietnam

* Corresponding author's e-mail: phancongngoc1402@gmail.com

Keywords: physicochemical properties, principal component analysis, statistical method, Pearson correlation analysis, The Nida valley

Abstract: The investigation of Nida Valley water aimed to assess fluctuations in physicochemical properties. In this study, environmental monitoring method was utilized to evaluate the changes in physicochemical properties of water. Over a 24-month period, from June 2021 to May 2023, a total of 228 water samples were collected from 10 sampling sites, with a monthly sampling frequency. Statistical analyses were utilized including the Shapiro–Wilk test ($\alpha = 0.05$), Kruskal–Wallis test and Wilcoxon (Mann–Whitney) rank sum test ($\alpha = 0.05$), Pearson correlation analysis ($\alpha = 0.001$) and principal component analysis (PCA). Statistical analyses revealed significant differences between months in GW samples for temperature, dissolved oxygen, pH, total nitrogen, total phosphorus, chloride, manganese, and zinc in GW samples and for T and DO in SW samples. Pearson correlation coefficient analysis ($\alpha = 0.001$) identified strong positive correlations within the SW dataset. Similarly, significant positive correlations were observed among the GW dataset. Noteworthy positive correlations were also detected between the GW and SW datasets. Principal component analysis (PCA) revealed a substantial dissimilarity between GW2 samples compared to others, characterized by elevated manganese, iron, and Sulfate content. Two distinct groups emerged: Group 1 included samples at GW1, GW2, GW3, GW5, and SW2, while Group 2 comprised all other samples. This study demonstrated the stability in the physicochemical properties of SW and underscore a discernible correlation between the hydrochemical compositions of both SW and GW in the riparian area. Outstanding characteristics in hydrochemical component of sample waters have been indicated.

Introduction

Water stands as an indispensable prerequisite for life. The requisite quality of water exhibits variability among individuals, alongside diverse criteria employed for evaluating its quality. Traditionally, the assessment of water quality involves a comparison of the physical and chemical attributes of a water sample against established guidelines or standards. It is imperative to note that water quality is not a static attribute of a system; rather, it cannot be encapsulated by the measurement of a singular parameter alone (Ayers and Westcot, 1985). Instead, it undergoes fluctuations in both temporal and spatial dimensions, necessitating regular monitoring to discern spatial patterns and temporal alterations.

An extensive array of chemical, physical, and biological components influencing water quality can be scrutinized, offering a broad indication of water pollution, while certain components enable the direct identification of pollution sources (Kowalik et al. 2015). Chemical pollutants emanate from industrial, domestic, and storm-related waste sources.

The contamination of water is culpable for the dissemination of diverse diseases (Bogdał et al. 2016), underscoring the need for monitoring water quality at multiple points along a watercourse. Additionally, when deemed necessary, treatment interventions are imperative to render contaminated water safe for human consumption. Mirabbasi et al. (2008) asserted that the appropriateness of water for diverse uses hinges on the type and concentration of dissolved minerals, which, in turn, are contingent upon the origin of river and groundwater sources. Recognized criteria for water quality requirements serve as guidelines for determining the suitability of water for diverse applications.

The evaluation of water resources mandates an understanding of water quality (Harmancioglu et al. 1998), emphasizing the significance of establishing a meticulously designed water quality monitoring network (Khalil et al. 2011). Typically, essential insights into water quality are derived from the analysis of water quality data. The term "water quality" encompasses the chemical, physical, and biological characteristics of water in relation to its suitability

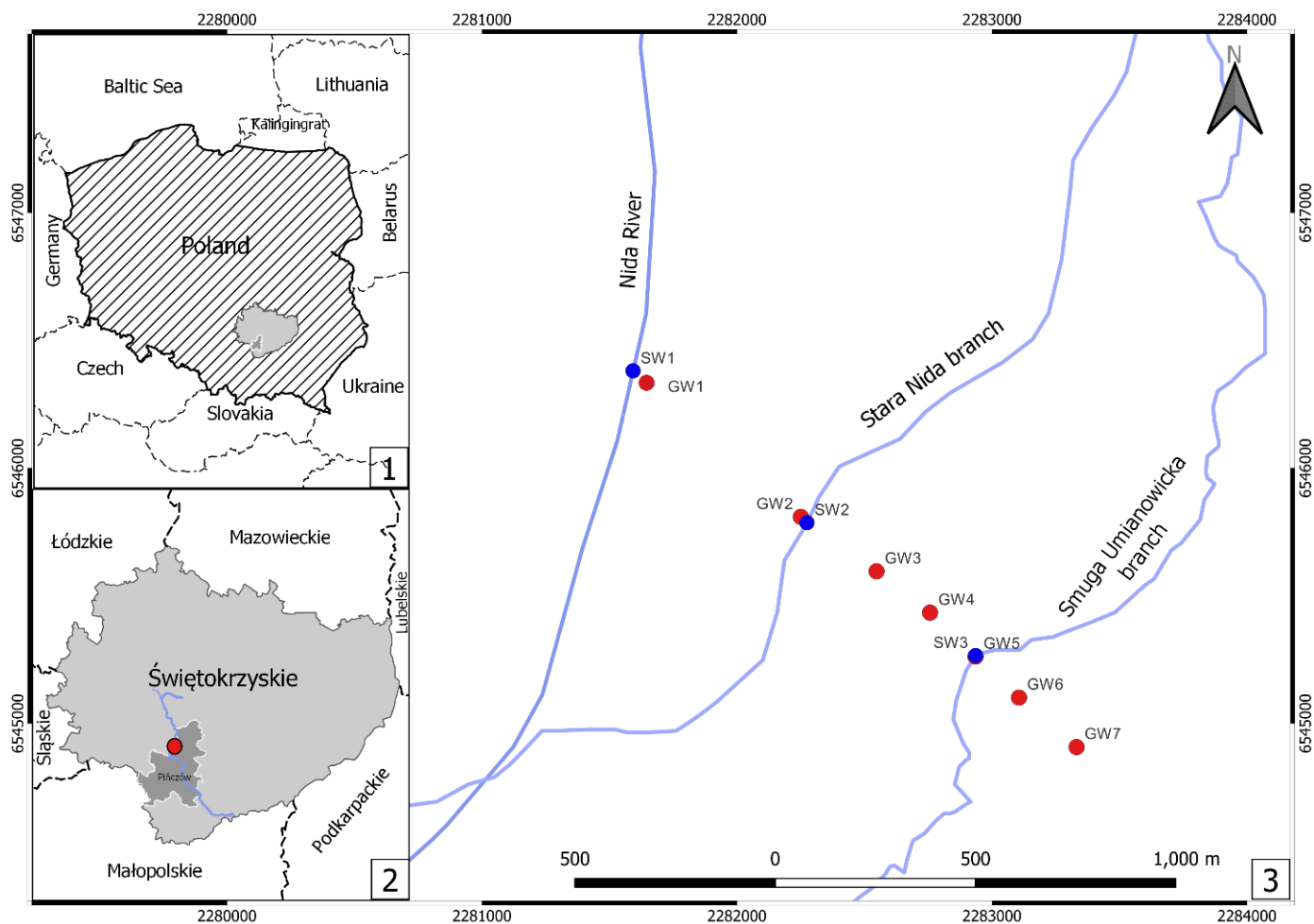


Figure 1. Map of study area and sampling sites in the Nida valley; source: own elaboration Explanation: Red points: groundwater collected locations. Blue points: water surface collected locations.

for a specific purpose (Chapman 1996). Consequently, water quality is contingent upon various factors, including the quality of recharge water and the nature of inputs from diverse sources (Schuh et al. 1997).

In this investigation, an environmental monitoring methodology was implemented to appraise the physicochemical attributes of both GW and SW. The characteristics of groundwater were ascertained through the collection of samples from strategically positioned monitoring wells (Vrana et al. 2005, Demaku and Bajraktari 2019). To ensure the robustness of the findings, these monitoring wells were strategically placed in close proximity, traversing through the contaminant plume, thereby enabling a multidimensional representation of the physicochemical components (Valett et al. 1990, Borden et al. 1997), facilitated by the use of multi-layered monitoring wells. A comprehensive network of these monitoring wells was established to furnish precise data regarding the spatial distribution of these components. In the case of surface water, the physicochemical indicators were delineated through the analysis of water samples obtained from diverse sources, including grab or bottle samples (Pitkin et al. 1999, Conant et al. 2004). However, this approach has its limitations, primarily offering only a snapshot of component levels at the time of sampling. Moreover, it demands a substantial volume of water sample, particularly when contaminants exist in trace amounts

(Vrana et al., 2005). To address these challenges effectively, automated sampling systems can be employed to enable continuous monitoring over extended durations.

The main goal of this study is to examine the physical and chemical characteristics of both SW and GW in the specific area under investigation. Furthermore, the study aims to evaluate how these characteristics change from month to month and compile a dataset that includes various physical and chemical indicators. This dataset will serve as a basis for future research projects in the same study area and policy makers can make accurate decisions for regional ecosystem conservation.

Materials and methods

Study area

The focal point of investigation is situated within the Nida Valley located in Poland. Encompassing a geographical expanse of 3,862.8 square kilometers, this river valley is characterized by extensive plains, lush grasslands, and waterlogged forests. The prevailing soil composition in this locale comprises a stratum of sand underlying a scant layer of mud. The genesis of the Nida Valley is attributable to the sinuous trajectory of the Nida River near the town of Pińczów. Within this topographical depression, three primary aquatic conduits exist. The central watercourse is the Nida River itself, extending over a distance

of 151.2 kilometers. The remaining bifurcations are the Smuga Umianowicka branch and the Stara Nida branch.

The course of the Nida River has undergone multiple modifications owing to flood control interventions. In specific segments, deliberate truncation of the river's course has been implemented. Commencing in the 1960s and extending into the early 20th century, endeavors were undertaken to regulate the flow of the Nida River, resulting in a reduction of its length. The original trajectory of the river, referred to as Stara Nida branch, was progressively shifted to the left, culminating in the formation of the contemporary Nida River. Nevertheless, downstream segments of the river maintain their inherent flow. These alterations have precipitated a diminution in the Nida Valley's natural ecological functionality, rendering it nearly desolate of water, with vestiges of erstwhile marshes and aquatic bodies persisting. This locale presents a distinctive opportunity to observe both the affirmative and adverse ramifications of historical flood control measures (Żelazo 1993, Łajczak 2004).

The specific study area is situated within the Nadnidziański Landscape Park and constitutes an integral component of a consequential ecological precinct (Strużyński et al. 2015). The floodplain within the Landscape experiences seasonal inundation, characterized by recurrent spring flooding and intermittent winter flooding, enduring for a span of 2 to 5 months annually and spanning a distance of 0.3 to 5 kilometers, proximate to the town of Umianowice. This floodplain serves as a pivotal natural reservoir for water, efficaciously diminishing the peril of riverine flooding (Borek and Drymajło 2019). As underscored by Łajczak (2004), this innate function of the floodplain assumes a pivotal role in regulating water levels and alleviating the incidence of inordinate flooding events.

Identification of sampling locations.

Ten meticulously chosen sampling points were established within the confines of the Nadnidziański Landscape Park. Among these, seven points were specifically designated as GW (GW1 to GW7) for the systematic collection of GW samples. These sampling locations comprise 2-meter-deep wells with a diameter of 10 centimeters, strategically drilled at cross-sections spaced every 150-200 meters. These wells, reinforced with plastic pipes, serve as purposeful and controlled sampling sites.

In addition, three distinct sampling points, denoted as SW, were strategically positioned within the aquatic environment. SW1 is situated at the Nida River, SW2 at the Stara Nida branch, and SW3 at the Smuga Umianowicka branch. The selection of these sampling points was methodically conducted along the Nida Valley, initiating from the regulated course of the Nida and extending through the Smuga Umianowicka branch, covering a linear distance of approximately 1365 meters from the primary channel of the river (refer to Figure 1).

Sample collection

A comprehensive dataset consisting of 228 water samples was systematically gathered throughout a 24-month period spanning from June 2021 to May 2023, with a consistent monthly sampling frequency. This extensive collection comprised 168 samples of GW and 60 samples from SW, procured from a total of 10 strategically designated sampling points. These points encompassed 7 locations earmarked for the collection of GW samples and 3 locations earmarked for

SW samples. Notably, for SW samples obtained from the Stara Nida branch, the sampling campaign exclusively occurred over a 12-month duration, from June 2022 to May 2023.

The sampling procedure involved the utilization of a vertical tube sampler equipped with a check valve, ensuring precision in sample extraction. The collected samples were promptly transferred into 300 cm³ bottles. To preserve their chemical and physical integrity, the samples underwent immediate transportation to the laboratory on the same day of collection. Subsequently, the samples were stored in a refrigerated environment at 4°C until further analysis. This meticulous approach was employed to maintain the quality and reliability of the collected water samples throughout the investigative process.

Field measurement

Physical indicators were determined right at the sample collection points using handheld devices. Oxygen meter (CO-411) was utilized for temperature (*T*) and dissolved oxygen (DO) measurements, while electrical conductivity (*EC*) was measured by conductivity meter (CC-102), pH was measured by pH meter (CP-104), and dissolved substances meter (TDS-3) was used for total dissolved solids (TDS) measurement.

To guarantee the precision of the readings, the instruments were meticulously calibrated in accordance with the manufacturer's specifications. This calibration process adhered to the recommended procedures, ensuring the accuracy and reliability of the acquired data. This rigorous calibration protocol was implemented to enhance the credibility and validity of the physical parameter measurements obtained during the study.

Laboratory analysis

Chemical indicators were analysed using the American Public Health Association (APHA 1998) and the Environmental Protection Agency (EPA 1983) methods in the laboratory.

Table 1. Limit of detection (LOD) and limit of quantitation (LOQ) for the parameters.

Parameter	Measurement unit	LOD	LOQ
TN	mg·dm ⁻³	0.05	0.05
TP	mg·dm ⁻³	0.005	0.01
Cu ²⁺	µg·dm ⁻³	0.5	1.00
Pb ²⁺	µg·dm ⁻³	0.5	1.00
Cd ²⁺	µg·dm ⁻³	0.5	1.00
Cl ⁻	mg·dm ⁻³	0.1	1.00
Fe ^{2+,3+}	mg·dm ⁻³	0.027	0.0743
Mn ²⁺	mg·dm ⁻³	0.009	0.027
Zn ²⁺	mg·dm ⁻³	0.0065	0.0198
SO ₄ ²⁻	mg·dm ⁻³	0.01	1.00

Source: own elaboration (based on laboratory equipment specifications)

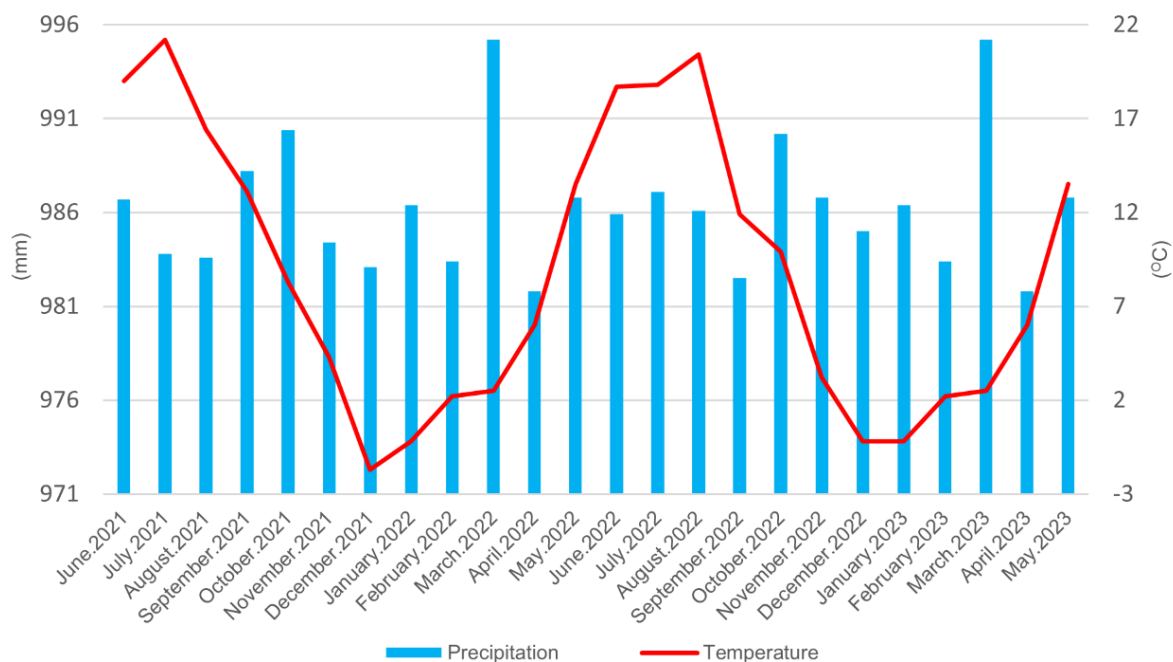


Figure 2. Annual mean values of temperature and precipitation in the study area; source: own elaboration based on data of IMGW – PIB. Available at: <https://hydro.imgw.pl>

Quantities of total nitrogen (TN) and total phosphorus (TP) were measured through the FiaCompact MLE flow analyser with mineralizer. The amount of $\text{Fe}^{2+,3+}$, Zn^{2+} , and Mn^{2+} was determined using the atomic absorption spectrometry (AAS) method with the Unicam Solar spectrophotometer at wavelengths 248.3 nm for $\text{Fe}^{2+,3+}$, 249.5 nm for Zn^{2+} and 213.9 nm for Mn^{2+} . Cd^{2+} , Cu^{2+} , and Pb^{2+} were measured using the EcaFlow analyser through the colorimetric method. The content of Cl^- was determined using the FiaSTAR analyser through the flow analysis method, while SO_4^{2-} was measured by the turbidimetric method. The method of titration using potassium permanganate was exploited for chemical oxygen demand (COD) measurement. Table 1 provides the detection limit (*LOD*) and quantitation limit (*LOQ*) of measurements. These standardized analytical methods were adhered to meticulously, ensuring the accuracy and reliability of the chemical parameter measurements in accordance with established protocols and guidelines.

Monitoring data and statistical analysis method

The normality of the variables was assessed using the Shapiro–Wilk test with a significance level (α) of 0.05. To discern significant differences in physicochemical parameters across different months, non-parametric analyses, including the Kruskal–Wallis test and Wilcoxon (Mann–Whitney) rank sum test at $\alpha = 0.05$, were conducted. Additionally, Pearson’s correlation coefficient (r) was employed to analyze correlation between the sampling points through hydrochemical parameters. A correlation matrix was constructed by computing coefficients for various pairs of sampling points, with significance determined based on the r -value and a significance level (p) of 0.001. Principal component analysis (PCA) was employed to elucidate the characteristics of monthly samples and identify hydrochemical parameters influencing each one.

Meteorological factors, specifically precipitation and air temperature, were monitored using data obtained

from the Kielce-Suków monitoring station via the website (<https://hydro.imgw.pl>). These data were utilized to explore correlations between changes in physicochemical parameters and meteorological factors. Monthly variations in precipitation and air temperature throughout the study period are depicted in Figure 2.

The statistical analysis was conducted using the R program, specifically version 4.1.2, which is open-source software operating under the GNU license. The analysis aimed to present key statistical parameters, including mean values, standard deviation, minimum, and maximum values. Emphasis was placed on capturing the monthly fluctuation of physicochemical parameters, providing a comprehensive understanding of the temporal variations in the dataset. This approach enables a robust exploration of the central tendencies and variability within the dataset across different months.

Results and Discussion

Fluctuations in physicochemical properties of surface water and groundwater

Physical properties

The physical parameters, including T, pH, EC, DO, and TDS, are depicted in Figure 3 for GW (on the left) and SW (on the right). Variations among different sampling months are indicated by the median values, as determined through the Kruskal–Wallis test and the Wilcoxon (Mann–Whitney).

Temperature: In this study, Kruskal–Wallis test was used to analyze the data for both GW and SW, revealing statistically significant differences in monthly temperature values. For GW, the test resulted in a chi-squared value of 146.02 with 11 degrees of freedom, yielding a p -value of less than $2.2e-16$. In the case of SW, the chi-squared value was 62.446 with 11 degrees of freedom, and the p -value was $3.247e-09$. Subsequently, the Wilcoxon test identified significant differences among the

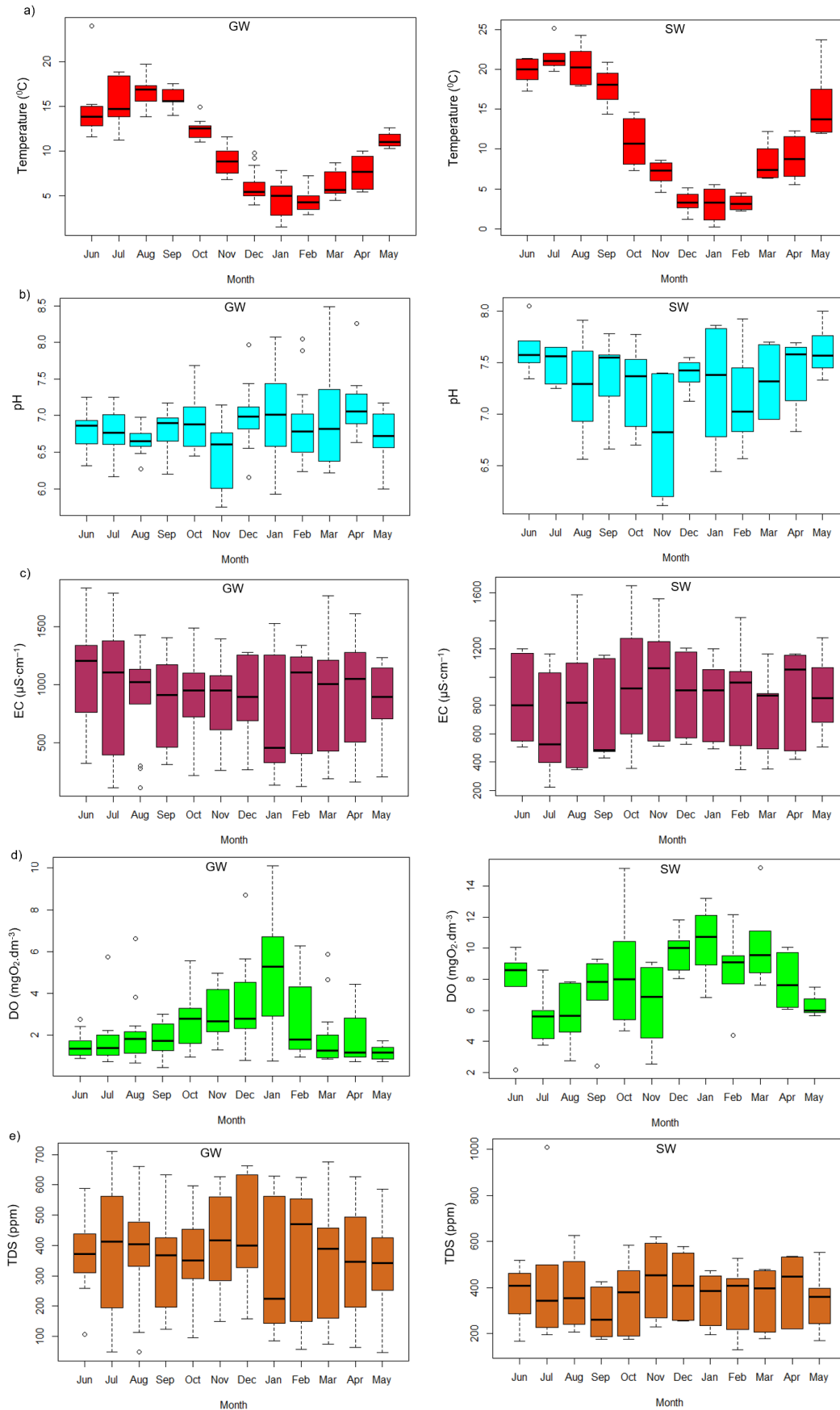


Figure 3. Monthly fluctuation in the physical parameters of GW and SW within the Nida Valley are illustrated in Figure 3. The parameters under investigation encompass: a) Temperature, b) pH, c) Electrical Conductivity (EC), d) Dissolved Oxygen (DO), and e) Total Dissolved Solids (TDS). Each parameter is depicted using a box-and-whisker plot in the graphical representation. The rectangles encapsulate the average values for each month, along with the corresponding standard deviation limits. The whiskers extend to denote the minimum and maximum values observed during the respective month. Any data points falling outside the whiskers, identified as outliers, are denoted by small circles. Source: Own Study.

following pairs of months for GW: June and July ($p = 0.028$), September and October ($p = 0.001$), October and November ($p = 0.001$), November and December ($p = 0.001$), December and January ($p = 0.012$), February and March ($p = 0.0001$), March and April ($p = 0.008$), April and May ($p = 0.0001$), and May and June ($p = 0.0001$). For SW, the Wilcoxon test indicated significant differences in the following pairs of months: October and November, November and December, and February and March, all with a p -value of 0.031. No other significant differences were observed in this context. Figure 3a illustrates the monthly temperature values of GW and SW. The findings presented above reveal a similarity in the monthly variations of water temperature between GW and SW. It is noteworthy, however, that the monthly temperature fluctuations in GW exhibit greater variability compared to those observed in SW. Water temperature is closely linked to ambient temperature and is significantly affected by seasonal changes (WHO 2017). This relationship explains the considerable rise in water temperature from June to September, corresponding to warmer seasons, and the subsequent decline in temperature during the colder months of December to February.

pH: The Kruskal–Wallis test (chi-squared = 21.727, $df = 11$, $p = 0.026$) conducted on the pH variable in GW revealed a statistically significant difference among the monthly pH values. Consequently, the Wilcoxon test identified significant differences among the following pairs of months: August and September ($p = 0.038$), November and December ($p = 0.016$), and April and May ($p = 0.001$). No significant differences were observed in other month pairs. In contrast, when applying the Kruskal–Wallis test (chi-squared = 13.133, $df = 11$, $p = 0.284$) to the pH data in SW, there was no statistically significant difference found among the monthly pH values. Figure 3b shows the monthly fluctuation in pH values of GW and SW. This observation indicates that the pH values in SW exhibit less month-to-month fluctuation compared to GW.

Electrical conductivity (EC): The Kruskal–Wallis test showed chi-squared = 6.0826, $df = 11$, $p = 0.8678$ for GW and chi-squared = 5.5751, $df = 11$, $p = 0.9002$ for SW. Thus, there were no statistically significant differences observed in the monthly EC values for both GW and SW. Figure 3c presents the monthly fluctuation in EC values of GW and SW. The results presented suggest a consistent stability in the hydrochemical composition of both SW and GW, with

no significant variations in water composition observed between different months. The observed variation in TDS resembled that of EC, with no statistically significant differences found in TDS values among different months for both GW and SW.

Dissolved oxygen (DO): The results of the Kruskal–Wallis test revealed statistically significant differences in DO values across months for both GW (chi-squared = 47.724, $df = 11$, $p = 1.599e-6$) and SW (chi-squared = 28.873, $df = 11$, $p = 0.002$). Subsequently, the Wilcoxon test identified significant differences in the following month pairs for GW: September and October ($p = 0.003$), January and February ($p = 0.029$), February and March ($p = 0.063$), and May and June ($p = 0.049$). In the case of SW, the Wilcoxon test also demonstrated significant differences between October and November, November and December, and March and April, all with a p -value of 0.031. No significant differences were observed in other month pairs. Figure 3d demonstrates the monthly fluctuation in DO values of GW and SW.

Chemical parameters

The chemical parameters including TP, TN, Cl^- , SO_4^{2-} , Mn^{2+} , $Fe^{2+,3+}$, Zn^{2+} , Pb^{2+} , Cd^{2+} , Cu^{2+} and COD are presented at Figure 4.

Total phosphorus (TP): In this analysis, the Kruskal–Wallis test was employed to assess the statistical significance of differences in TP values across months for GW, revealing a notable result (chi-squared = 23.903, $df = 11$, $p = 0.013$). Specifically, the Wilcoxon test identified significant distinctions among the following month pairs: November and December ($p = 0.025$), December and January ($p = 0.008$), January and February ($p = 0.01$), and May and June ($p = 0.004$). Notably, no other significant differences were observed in the pairs. Conversely, when analyzing the monthly TP values for SW, the Kruskal–Wallis test indicated no statistically significant variation (chi-squared = 13.844, $df = 11$, $p = 0.241$). Figure 4a shows the monthly fluctuation in TP values of GW and SW. This result indicates that the measured value of monthly TP in SW is more stable than that in GW.

Total nitrogen (TN): The result of the Kruskal–Wallis test (chi-squared = 27.061, $df = 11$, $p = 0.004$) indicates a statistically significant difference in the monthly TN values for GW. Subsequently, the Wilcoxon test further confirmed these

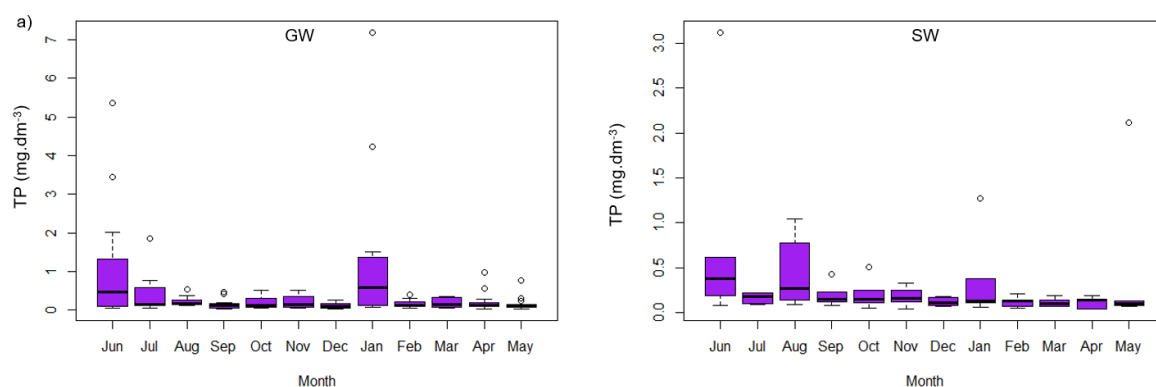


Figure 4. Monthly fluctuation in chemical parameter of GW and SW in the Nida valley: a) total phosphorus (TP), b) total nitrogen (TN), c) chloride (Cl^-), d) sulphate (SO_4^{2-}), e) manganese (Mn^{2+}), f) iron ($Fe^{2+,3+}$), g) zinc (Zn^{2+}), h) cadmium (Cd^{2+}), i) lead (Pb^{2+}), j) copper (Cu^{2+}), k) chemical oxygen demand (COD); Source: Own Study.

Figure 4.

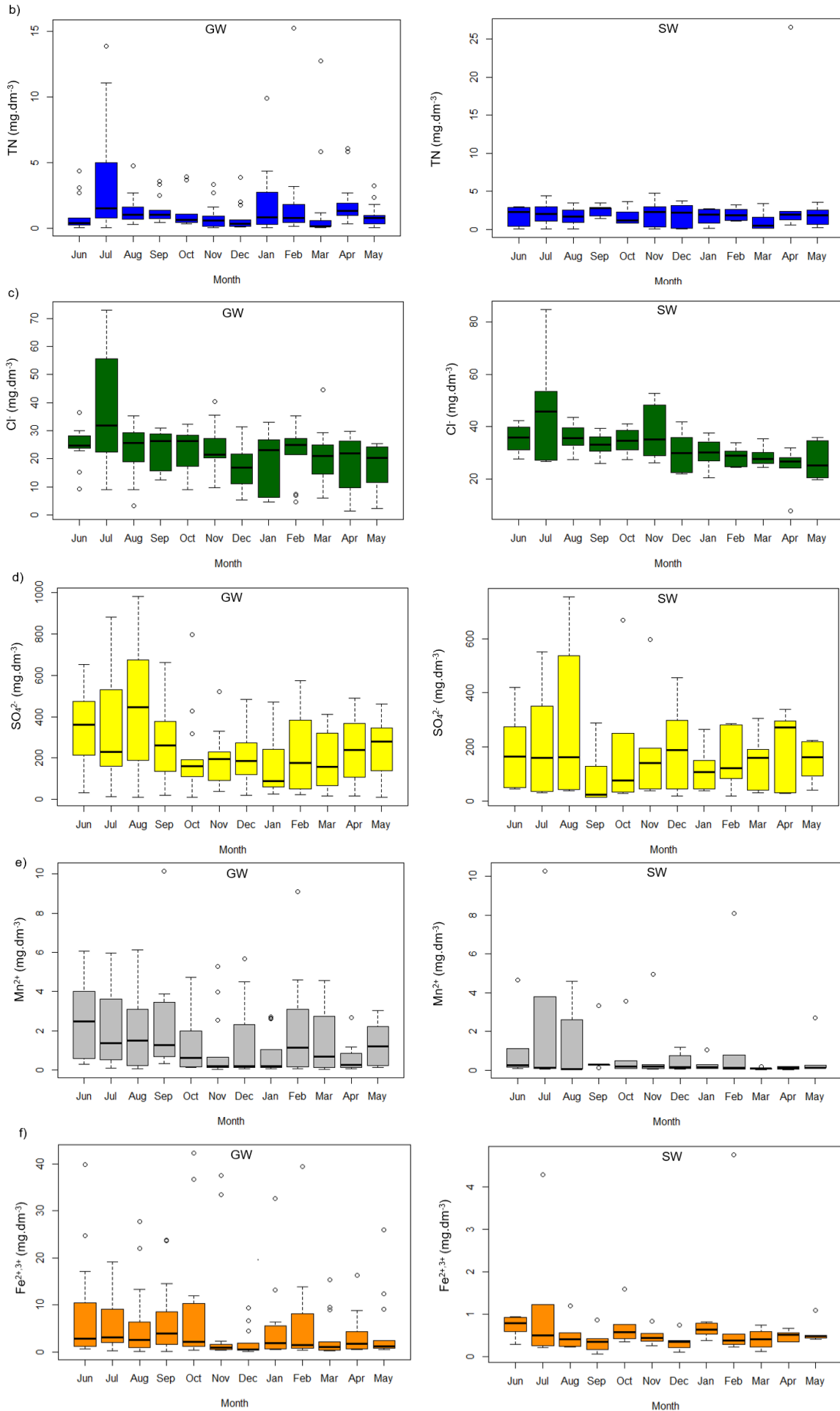
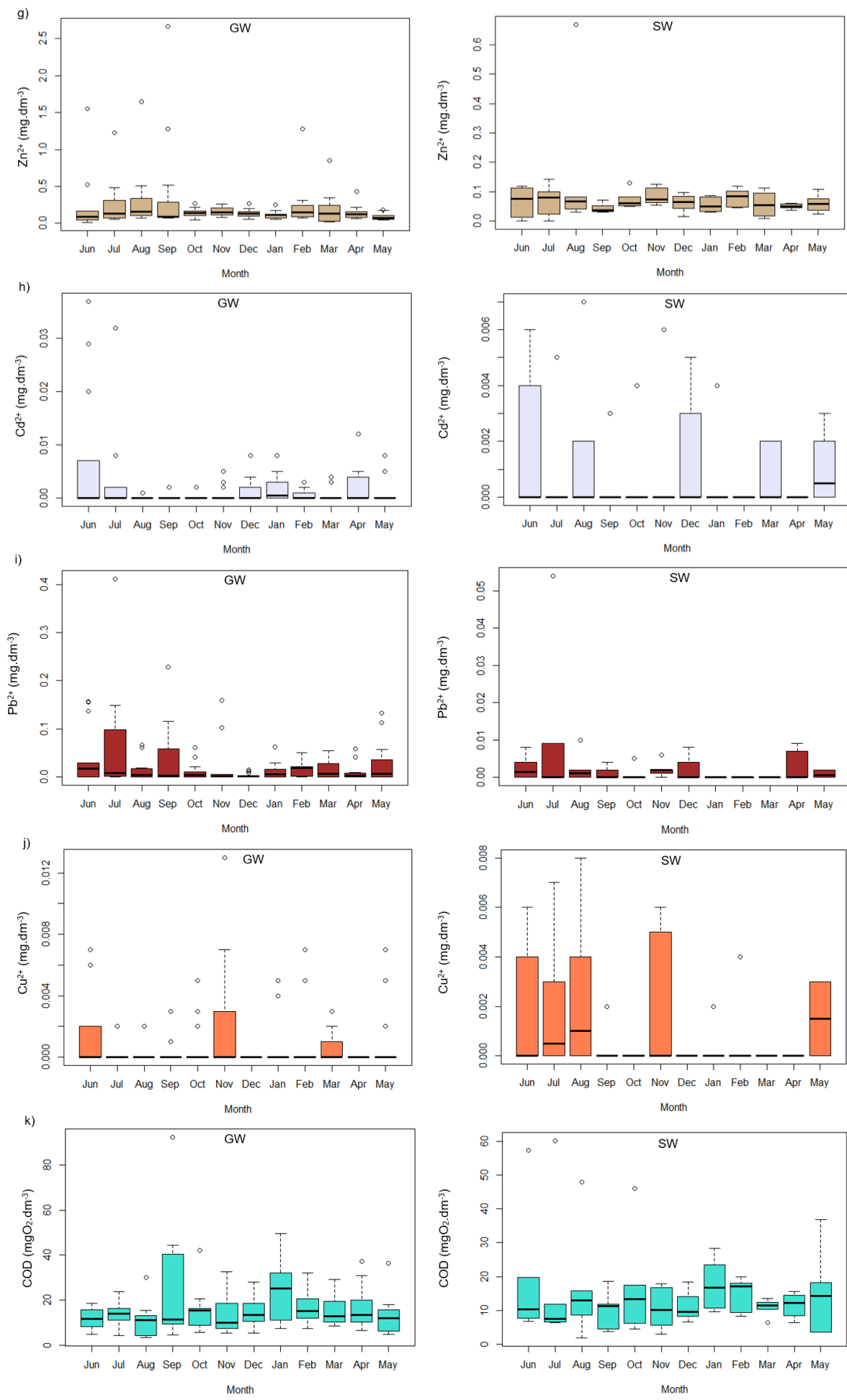


Figure 4.



distinctions, highlighting significant differences among the following month pairs: June and July ($p = 0.02$), December and January ($p = 0.006$), February and March ($p = 0.049$), and April and May ($p = 0.005$). It is worth noting that no other significant differences were observed in the other pairs for GW. Conversely, when assessing the monthly TN values for SW, the Kruskal–Wallis test revealed no statistically significant differences (chi-squared = 4.7913, $df = 11$, $p = 0.94$). Figure 4b indicates the monthly fluctuation in TN values of GW and SW. This means that the TN composition in SW measured monthly is less variable than in GW.

Chloride (Cl^-): The Kruskal–Wallis test (chi-squared = 19.267, $df = 11$, $p = 0.035$) revealed a statistically significant difference in the monthly Cl^- values for GW. Further analysis using the Wilcoxon test highlighted significant distinctions between specific month pairs, including July and August ($p = 0.008$), November and December ($p = 0.001$), May and June ($p = 0.003$). No other statistically significant differences were observed in the Cl^- values for GW. In contrast, when examining the monthly Cl^- values for SW, the Kruskal–Wallis test (chi-squared = 20.803, $df = 11$, $p = 0.056$) showed no statistically significant differences. Figure 4c illustrates the monthly fluctuation in Cl^- values of GW and SW.

Manganese (Mn^{2+}): The Kruskal–Wallis test for Mn^{2+} in GW revealed a chi-squared value of 24.192 ($df = 11$, $p = 0.011$), signifying statistical differences in the monthly Mn^{2+} values. Subsequent analysis with the Wilcoxon test indicated a significant difference only between September and October ($p = 0.017$). No other statistically significant differences were observed in the pairs of month. Conversely, when examining the monthly Mn^{2+} values for SW, the Kruskal–Wallis test returned a chi-squared value of 12.32 ($df = 11$, $p = 0.34$), indicating that there were no statistically significant differences among the monthly Mn^{2+} values. Figure 4e presents the monthly fluctuation in SO_4^{2-} values of GW and SW.

Zinc (Zn^{2+}): The Kruskal–Wallis test (chi-squared = 18.835, $df = 11$, $p = 0.044$) indicated a statistical difference in the monthly Zn^{2+} values for GW. Further analysis using the Wilcoxon test revealed significant differences among specific month pairs, including November and December ($p = 0.049$), January and February ($p = 0.006$), and April and May ($p = 0.041$). However, no other significant differences were observed among the remaining pairs of months in GW. In contrast, when assessing the monthly Zn^{2+} values for SW, the Kruskal–Wallis test (chi-squared = 8.442, $df = 11$, $p = 0.673$) showed no statistically significant differences. Figure 4g displays the monthly fluctuation in Zn^{2+} values of GW and SW. The obtained results show that the Zn^{2+} composition in GW measured monthly changes more than that in SW.

The Kruskal–Wallis test results indicate no statistically significant differences in the monthly values of SO_4^{2-} , $Fe^{2+,3+}$, Cd^{2+} , Pb^{2+} , Cu^{2+} , and COD for both GW and SW. Specifically, for SO_4^{2-} : 17.739, $df = 11$; $Fe^{2+,3+}$: 19.776, $df = 11$; Cd^{2+} : 18.258, $df = 11$; Pb^{2+} : 13.712, $df = 11$; Cu^{2+} : 18.415, $df = 11$; COD: 18.138, $df = 11$) and SW (SO_4^{2-} : 4.984, $df = 11$; $Fe^{2+,3+}$: 13.361, $df = 11$; Cd^{2+} : 6.966, $df = 11$; Pb^{2+} : 15.284, $df = 11$; Cu^{2+} : 17.709, $df = 11$; COD: 6.688, $df = 11$), with p-values

ranging from 0.058 to 0.931. Figures 4d, 4f, 4h, 4i, 4j, 4k respectively display the monthly values of SO_4^{2-} , $Fe^{2+,3+}$, Cd^{2+} , Pb^{2+} , Cu^{2+} , and COD in both GW and SW.

Correlation between hydrochemical components of surface water and groundwater

Pearson's correlation coefficient analysis method

The hydrochemical parameters selected for these analytical methods encompass TP, TN, Mn^{2+} , $Fe^{2+,3+}$, Zn^{2+} , SO_4^{2-} and Cl^- . Figure 5 depicts correlation coefficients (r) illustrating the monthly variations in hydrochemical composition for both surface water (SW) and groundwater (GW) at sampling points. These coefficients are presented in the correlation matrix, accompanied by their corresponding significance levels (p-values). In all instances, a positive correlation was identified, with correlation coefficients (r) exceeding 0.5 and p-values less than 0.001.

Notably, strong positive correlations were identified within the SW dataset (comprising SW1, SW2, and GW3), exhibiting correlation coefficients ranging from 0.87 to 0.94. Moreover, significant positive correlations were observed among the GW dataset (encompassing GW1, GW2, GW3, GW4, GW5, GW6, and GW7), with correlation coefficients ranging from 0.64 to 0.92. Additionally, noteworthy positive correlations were detected between the GW and SW datasets, with correlation coefficients falling between 0.78 and 0.94.

The findings from this study highlight a discernible correlation between the hydrochemical compositions of both SW and GW in the riparian area. These correlations, characterized by an elevated concentration of dissolved minerals, can be attributed to rock weathering processes, as previously suggested by Costello et al. (1984) and Nowobilska-Luberda (2018).

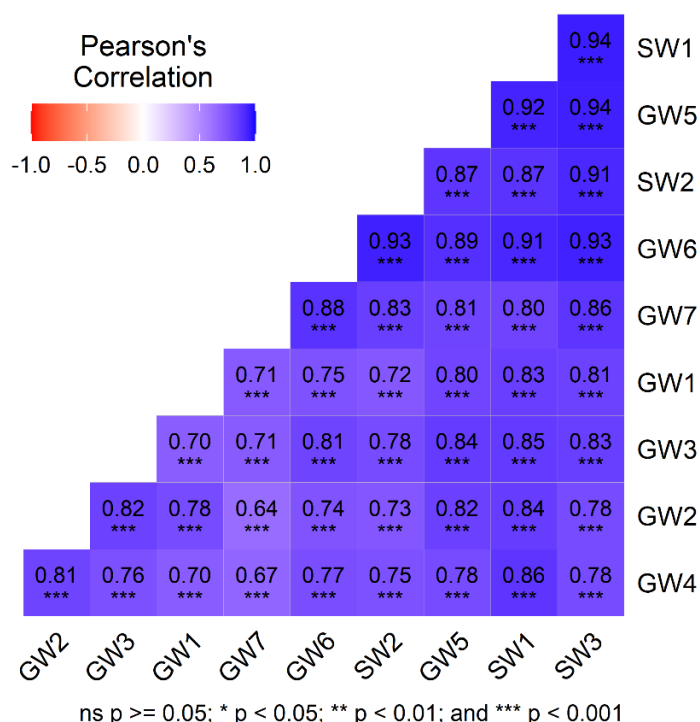


Figure 5. Correlation matrix of the hydrochemical properties at the observed points.

Particularly, the hydrochemical composition of GW within the riparian area reveals a robust correlation, indicative of the exchange of GW between observation points throughout the study area. This phenomenon can be elucidated by the unique topography of the Nida valley, which is a lowland area prone to prolonged flooding for many months. As a result, both the water exchange process and material transport process are intensified, as discussed by Żelazo (1993), Łajczak (2004), and Strużyński et al. (2015). Additionally, research conducted by Phan et al. (2023) concerning GW in the Nida valley has brought to light significant concentrations of Mn^{2+} and $Fe^{2+,3+}$. The physicochemical analysis conducted in this study indicates that these elements are present at notably high levels. Furthermore, the research underscores the existence of seasonal variations in GW properties, with the content of various compounds being particularly elevated during the summer and lower during other seasons.

Furthermore, a robust correlation exists between the hydrochemical compositions of SW and GW. This correlation can be attributed to the dilution or addition of compounds as the stream traverses diverse regions, resulting in heterogeneous changes in the hydrochemical properties of SW. This phenomenon characterizes the flowing area, as noted by Demaku and Bajraktari in 2019. Moreover, a strong correlation in the hydrochemical composition is observed among SW in the Nida River (SW1), the Stara Nida branch (SW2), and the Smuga Umianowicka branch (SW3). This correlation can be explained by the interconnection of these three streams, with the two branches, Smuga Umianowicka and Stara Nida, originating from the main flow of the Nida River. All three of these streams traverse the Nida valley, and their hydrochemical composition is characteristic of this region, as discussed by Cel et al. in 2017 and Phan et al. in 2023. Additionally, Wojak et al. (2023), in their investigation have conducted measurements and simulations on a segment of the Nida River. Their research revealed the existence of complex relationships between water flow and the riverbed. Variations in river discharge not only impact the magnitude of flow processes but also influence water composition.

Outstanding characteristics in hydrochemical component of water

Principal Component Analysis (PCA) method

The results of Principal Component Analysis (PCA) identified four key factors, collectively explaining 74.7% of the total variance. These results are visually presented in the PCA-biplot, where Dimension 1 (Dim1) accounts for 27.6% and Dimension 2 (Dim2) for 16.4% in Figure 6a, while Dimension 3 (Dim3) represents 16.1% and Dimension 4 (Dim4) accounts for 14.6% in Figure 6b.

Dim1 exhibited negative loadings for all parameters, including TP, TN, Mn^{2+} , $Fe^{2+,3+}$, Zn^{2+} , SO_4^{2-} and Cl^- . Notably, among these variables, Mn^{2+} , SO_4^{2-} , and $Fe^{2+,3+}$ displayed the strongest negative loadings compared to the others. Therefore, a decrease in Mn^{2+} , SO_4^{2-} , and $Fe^{2+,3+}$ levels is likely to correspond to an increase in the other parameters. Furthermore, Dim1 revealed distinct differences among samples, particularly for July at GW2 (point No. 9), August at GW2 (point No. 15), and June at GW2 (point No. 83) in comparison to the other samples. Dim1 also highlights two distinct groups of samples.

Group 1 includes samples with high Mn^{2+} , $Fe^{2+,3+}$, and SO_4^{2-} content, such as numbers 2, 9, 15, 34, 83, 90, 97, 139 (June, July, August, November, February at GW2), numbers 8 and 103 (July and September at GW1), numbers 22, 105, 133, 140 (September, June, February at GW3), number 85 (June at GW4), number 142 (February at GW5), and numbers 176 and 217 (July and February at SW2). Group 2 includes all other sample numbers.

Dim2 displayed positive loadings for TN, TP, and Cl^- , and negative loadings for $Fe^{2+,3+}$, SO_4^{2-} and Zn^{2+} . The variation in TN showed the strongest positive loading, while the variation in $Fe^{2+,3+}$ showed the strongest negative loading compared to the other variables. Consequently, an increase in TN levels is likely to be associated with an increase in the other parameters, while a decrease in $Fe^{2+,3+}$ levels may lead to an increase in the other parameters. Dim2 also revealed significant differences between samples, particularly for July at GW5 (point No. 12), July at GW6 (point No. 13), February at GW1 (point No. 54), September at GW1 (point No. 103), July at SW1 (point No. 172), and April at SW3 (point No. 227), attributed to high TN content.

Dim3 exhibited negative loadings for TN, Zn^{2+} , $Fe^{2+,3+}$, Mn^{2+} , and positive loadings for TP, SO_4^{2-} and Cl^- . Notably, the most substantial positive loading was observed for Zn^{2+} , suggesting that an increase in Zn^{2+} would likely result in an increase in the other parameters. Dim3 also highlighted distinct differences between September at GW2 (point No. 21) and September at GW1 (point No. 103) in comparison to others, characterized by high TN content at GW1 and high Zn^{2+} content at GW2.

Dim4 displayed negative loadings for TP, Zn^{2+} and Cl^- , and positive loadings for TN, $Fe^{2+,3+}$, Mn^{2+} and SO_4^{2-} . Particularly, the most prominent negative loading was associated with TP, indicating that a decrease in TP levels would likely lead to an increase in the other parameters. Dim4 revealed significant differences between samples, especially for January at GW2 (point No. 48) and at GW3 (point No. 49), June at GW4 (point No. 4), at GW5 (point No. 5), at GW1 (point No. 1), and at SW1 (point No. 166), characterized by high TP content at GW1 to GW5 and high Zn^{2+} content at SW1. In addition, Dim4 indicated a high degree of similarity among the remaining samples.

Conclusions

This investigation provides comprehensive insights into the physicochemical characteristic of water in the Nida Valley, Poland, throughout the study period.

The study results revealed significant differences among months for temperature, dissolved oxygen, pH, total nitrogen, total phosphorus, chloride, manganese, and zinc in GW samples and for *T* and DO in SW samples. This suggests the stability of the physicochemical properties of SW when compared to GW in the study area.

Significant positive correlation in chemical composition changes between GW sampling points and between SW sampling points. Noteworthy positive correlations were also detected between the GW and SW sampling points. The study findings underscore a discernible correlation between the hydrochemical compositions of both SW and GW in the riparian area.

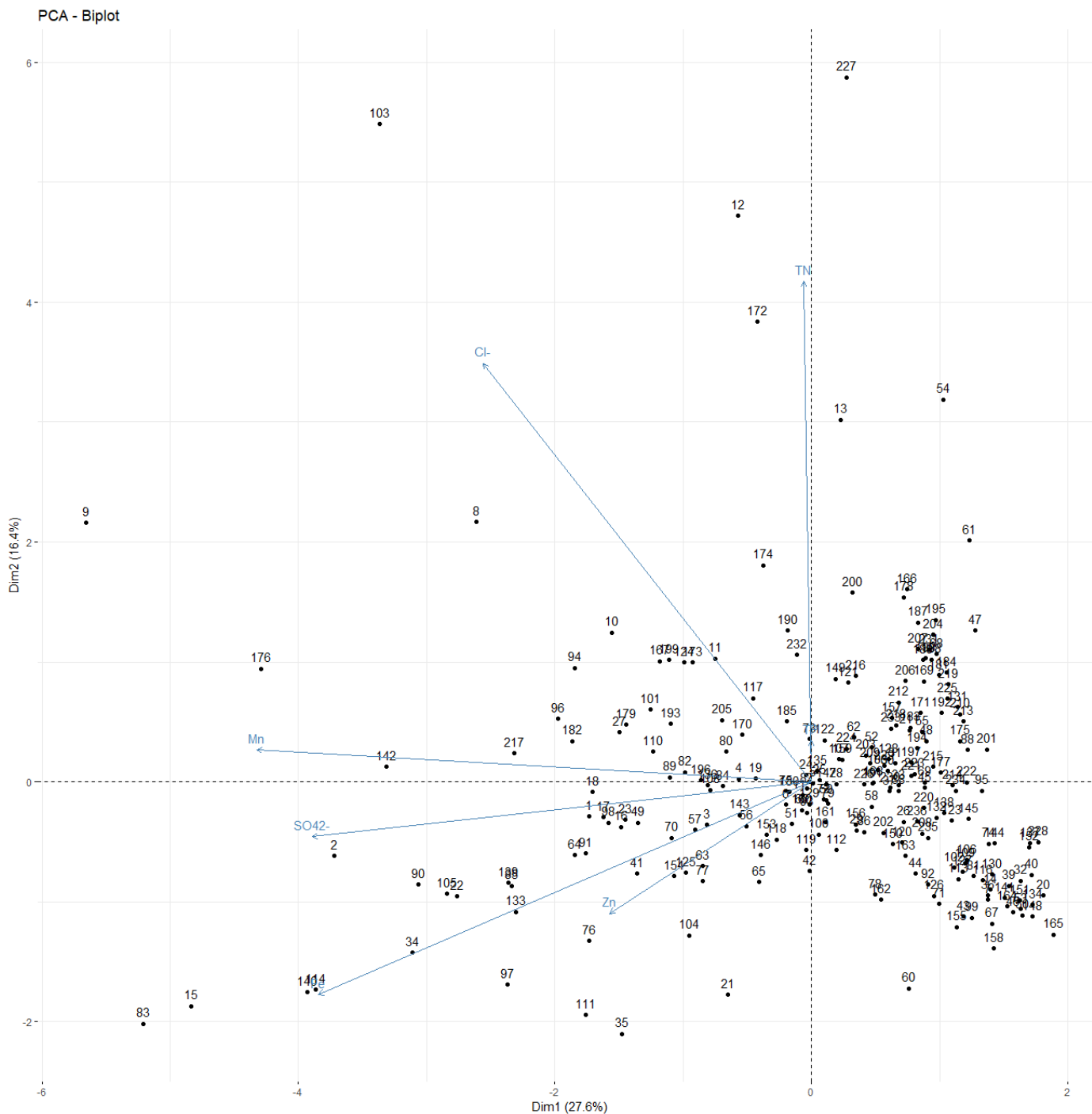


Figure 6a. Biplot – resulting from the principal component analysis: source: own study.

The dissimilarity among GW2 samples compared to others was revealed, characterized by elevated Mn^{2+} , $Fe^{2+,3+}$, and SO_4^{2-} content. Two distinct groups emerged: Group 1 included samples at GW1, GW2, GW3, GW5, and SW2, while Group 2 comprised all other samples. Significant differences among samples were noted, particularly for July at GW5 and GW6, February and September at GW1, July at SW1, and April at SW3, attributed to high TN and Zn^{2+} content at GW2 and SW1. Additionally, it presented a character of high TP content at GW1 to GW5.

The obtained results are consistent and reliable. This study is ongoing, the data will be supplemented and completed. The data can be used as reference data for water studies in the Nida valley.

References

- APHA (1998). Standard methods for the examination of water and wastewater. 20th ed. Washington, DC. American Public Health Association. ISBN 0875532357 pp. 1325
- Ayers, R.S. & Westcot D.W. (1985). Water quality for agriculture. FAO Irrigation and Drainage Paper No. 29, Rome, Italy, pp: 8-96. ISBN 92-5-102263-1
- Bogdał, A., Kowalik, T., Ostrowski, K. & Skowron P. (2016). Seasonal variability of physicochemical parameters of water quality on length of Uswicza river, *J. Ecol. Eng.* 17(1), pp. 161–170. DOI:10.12911/22998993/61206
- Borden, R.C., Daniel, R.A., LeBrun, L.E. & Davis, C.W. (1997).

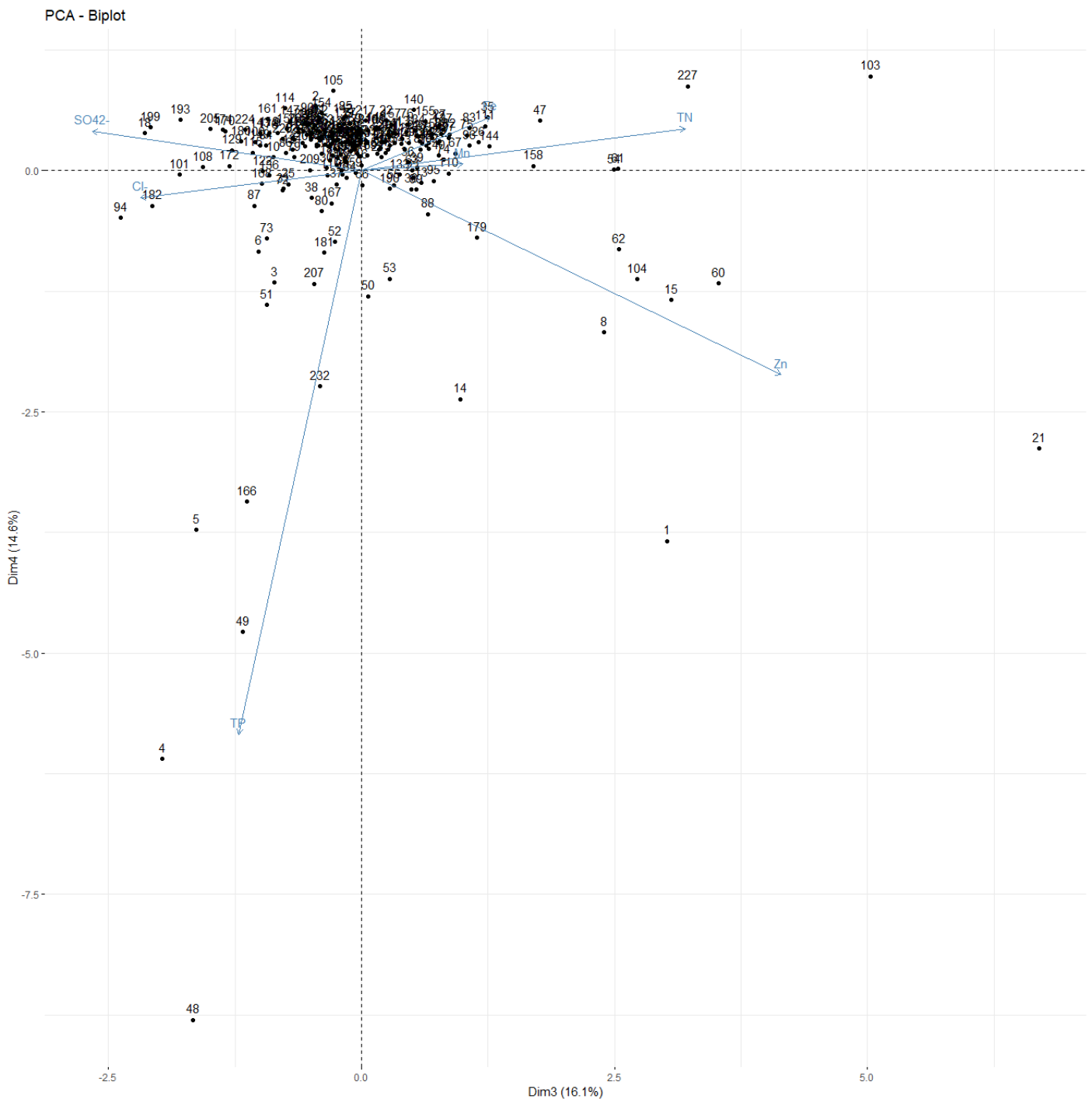


Figure 6b.

Intrinsic biodegradation of MTBE and BTEX in a gasoline-contaminated aquifer, *Water Resour. Res.* 33, 1105–1115. DOI:10.1029/97W.R00014

Borek, Ł. & Drymajło K. (2019). The role and importance of irrigation system for increasing the water resources: the case of the Nida River valley, *ASP.FC.* 18, 19–30. DOI:10.15576/ASP.FC/2019.18.3.19

Cel, W., Kujawska, J. & Wasąg H. (2017). Impact of hydraulic fracturing on the quality of natural waters, *J. Ecol. Eng.* 18, pp. 63–68. DOI:10.12911/22998993/67852

Chapman, D.V. (1996). *Water Quality Assessments: A Guide to the Use of Biota, Sediments and Water in Environmental Monitoring.* 2nd Edn., Taylor and Francis, London, UK., pp: 626. ISBN-13: 9780419215905.

Conant, B., Cherry, J.A. & Gillham, R.W. (2004). A PCE groundwater plume discharging to a river: influence of the streambed and near-river zone on contaminant distributions, *Journal of Contaminant Hydrology* 73, pp. 249–279. DOI:10.1016/j.jconhyd.2004.04.001

Costello, M.J., McCarthy, T.K. & O'Farrell M.M. (1984). The stoneflies (Plecoptera) of the Corrib catchment area, Ireland, *Annls Limnol.* 20, 25–34. DOI:10.1051/limn/1984014

Demaku, S. & Bajraktari, N. (2019). Physicochemical Analysis of the Water Wells in the Area of Kosovo Energetic Corporation (Obiliq, Kosovo), *J. Ecol. Eng.* 20, pp. 155–160. DOI:10.12911/22998993/109874

EPA (1983). *Methods for chemical analysis of water and wastes.* Washington, DC. United States Environmental Protection Agency pp. 491

- Harmancioglu, N.B., Ozkul, S.D. & Alpaslan, M.N. (1998). Water Quality Monitoring and Network Design. [In:] Harmancioglu, N.B., Singh, V.P., Alpaslan, M.N. (eds) Environmental Data Management, Water Science and Technology Library, vol 27. Springer, Dordrecht. DOI:10.1007/978-94-015-9056-3_4
- Khalil, B., Ouarda, T.B.M.J. & St-Hilaire, A. (2011). Estimation of water quality characteristics at ungauged sites using artificial neural networks and canonical correlation analysis, *J. Hydrol.*, 405, pp. 277-287. DOI:10.1016/j.jhydrol.2011.05.024
- Kowalik, T., Bogdał, A., Borek, Ł. & Kogut, A. (2015). The effect of treated sewage outflow from a modernized sewage treatment plant on water quality of the Breń River, *J. Ecol. Eng.* 16, pp. 96–102. DOI:10.12911/22998993/59355
- Łajczak, A. (2004). Negative consequences of regulation of a meandering sandy river and proposals tending to diminish flood hazard. Case study of the Nida river, southern Poland. Proceedings of the Ninth International Symposium on River Sedimentation. Yichang, China. Beijing. IAHR p. 1773–1783
- Mirabbasi, R., Mazloumzadeh, S.M. & Rahnama, M.B. (2008). Evaluation of irrigation water quality using fuzzy logic, *Res. J. Environ. Sci.*, 2, pp. 340-352. DOI:10.3923/rjes.2008.340.352
- Nowobilaska-Luberda, A. (2018). Physicochemical and Bacteriological Status of Surface Waters and Groundwater in the Selected Catchment Area of the Dunajec River Basin, *J. Ecol. Eng.* 19, pp. 162–169. DOI:10.12911/22998993/86329
- Phan, C.N., Strużyński, A. & Kowalik, T. (2023). Monthly changes in physicochemical parameters of the groundwater in Nida valley, Poland (case study). *Journal of water and Land development*, 56 (I–III), pp. 220–234. DOI:10.24425/jwld.2023.143763
- Pitkin, S.E., Cherry, J.A., Ingleton, R.A. & Broholm M. (1999). Field Demonstrations Using the Waterloo Ground Water Profiler, *Ground Water Monit. Remediat* 19, pp. 122–131. DOI:10.1111/j.1745-6592.1999.tb00213.x
- Schuh, W.M., Klinkebiel, D.L., Gardner, J.C. & Meyer, R.F. (1997). Tracer and nitrate movement to groundwater in the northern great plains, *J. Environ. Qual.*, 26, pp. 1335-1347. DOI:10.2134/jeq1997.00472425002600050020x
- Strużyński, A., Książek, L., Bartnik, W., Radecki-Pawlik, A., Plesiński, K., Florek, J., Wyrębek, M. & Strużyński M. (2015). Wetlands in River Valleys as an Effect of Fluvial Processes and Anthropopression, [in:] Ignar, S., Grygoruk, M. (Eds.), *Wetlands and Water Framework Directive*, GeoPlanet: Earth and Planetary Sciences, Springer International Publishing, Cham, pp. 69–90. DOI:10.1007/978-3-319-13764-3_5
- Valett, H.M., Fisher, S.G. & Stanley, E.H. (1990). Physical and Chemical Characteristics of the Hyporheic Zone of a Sonoran Desert Stream, *Journal of the North American Benthological Society* 9, pp. 201–215. DOI:10.2307/1467584
- Vrana, B., Allan, I.J., Greenwood, R., Mills, G.A., Dominiak, E., Svensson, K., Knutsson, J. & Morrison G. (2005). Passive sampling techniques for monitoring pollutants in water, *TrAC Trends in Analytical Chemistry* 24, pp. 845–868. DOI:10.1016/j.trac.2005.06.006
- WHO (2017). Guidelines for drinking-water quality [online]. 4th ed. World Health Organization ISBN 9789241548151 pp. 541. [Access 10.06.2022]. Available at: <https://apublica.org/wp-content/uploads/2014/03/Guidelines-OMS-2011.pdf>
- Wojak, S., Strużyński, A. & Wyrębek M. (2023). Analysis of changes in hydraulic parameters in a lowland river using numerical modeling, *ASP.FC* 22, pp. 3–17. DOI:10.15576/ASP.FC/2023.22.1.3
- Żelazo, J. (1993). The recent views on the small lowland river training. [In:] *Nature and environment conservation in the lowland river valleys in Poland*. Ed. L. Tomiałojć. Kraków. IOP PAN p. 145–154 (in Polish)